

## 4 Mathematical process model

This chapter deals with the different aspects of the process model developed within the scope of this thesis. As depicted in fig. 4.1 In the case of cryogenic air separation three main tasks for the process can be identified. These are the compression of raw materials, heat exchange with product streams and the separation of air. While those different stages are highly interdependent they will be discussed separately and mathematical models for the main process units will be presented.

The first section (sec. 4.1) deals with a steady state version of the process model. Especially for steady state models the issue of initializing the variables in such a way that the solver can converge to a solution becomes crucial. With that in mind the strategies developed to initialize in particular the distillation columns will be elaborated upon within that first section as well.

The second section (sec. 4.2) is devoted to a dynamic version of the models for some process units. In addition to the models themselves several aspects which arise, when considering process dynamics will also be part of that section.

In the third section (sec. 4.3) of this chapter takes a closer look at how the economics of the process can be captured during process simulation. Understandably, the issue of economic evaluation is closely tied to the sizing of each process unit and with that also to the operational boundaries of the process equipment. As these aspects are for the most part treated uniformly for the steady state case and dynamic case the will be dealt with in a single section.

All presented models have been implemented in the equation based process simulator gPROMS®. Certain aspects arising when implementing the models will be discussed in the last section of this chapter sec. 4.5.

### 4.1 Steady - state unit models

#### 4.1.1 Separation

Distillation columns are among the most widely studied pieces of process equipment. While much

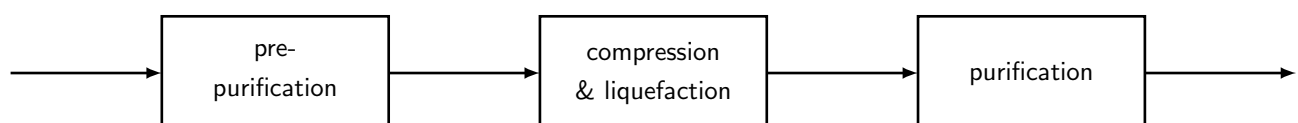


Figure 4.1: simplified cryogenic air separation process.

briefly  
discuss  
general  
process  
steps.  
men-  
tion  
pre-  
purificat

find  
appro-  
priate  
place  
for in-  
teg-  
rated  
reboiler  
con-  
denser  
unit.

add

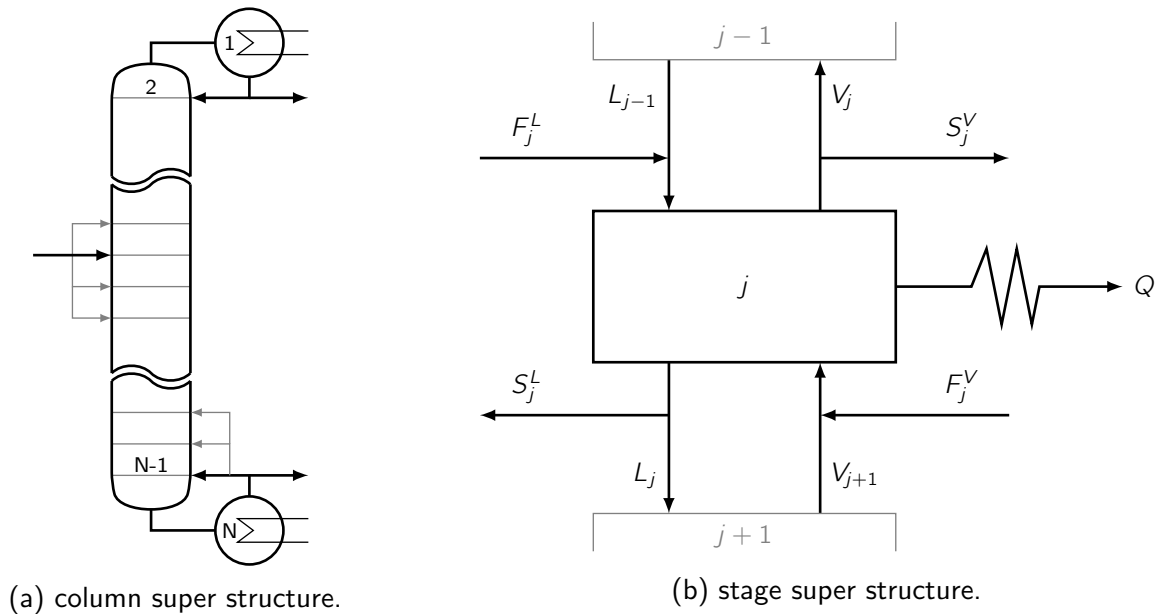


Figure 4.2: superstructures for column and column stages.

has been accomplished, the robust simulation poses great challenges to this day. In the context of cryogenic air separation the associated mixture displays only moderate non-idealities and furthermore is a zeotropic one. However further complexity is added due to the strong interdependencies of the different columns arising from thermal and material coupling within the process.

In this section first the mathematical formulation for a general steady-state distillation column model will be presented (sec. 4.1.1). The

### Distillation column model

In this section the working equations used to model the different distillation columns in the process, known as the MESH equations, are given. These equations, although rather plain at first glimpse, form a set of highly non-linear, highly coupled equations. The solutions of these equations is not a trivial task for current solution algorithms, whose success is highly dependent on the quality of initial guesses provided. Therefore a strategy used for the automated generation of such guesses will be described as well.

The model presented here is not only to be used for the simulation of of a given process, but rather for optimization purposes as well. While several of the continuous decision variables associated with process optimization can be optimized from a generic set of equations, others need further consideration. The optimization decision which adds the greatest complexity for distillation columns is the number of trays used in a given separation process. This introduces integer decisions into the model and requires development of a super structure to be used.

The starting point for the modeling a distillation column is considering a single separation stage within the column with all possible connections. Fig. 4.2a shows the superstructure to be used for the complete column, while fig. 4.2b shows a super structure for a single stage.

add  
side  
draws  
to  
column  
super  
struc-  
ture

As mentioned before the governing equations for a distillation column are known as MESH equations. The acronym MESH stands for material, equilibrium, summation and enthalpy. The corresponding equations are as follows. If not stated otherwise, all equations presented in this section are true for all stages. In order to improve readability the indices denoting a stage are omitted, if not essential for the meaning of a given equation. For all equations the number of stages in the process is denoted by  $n_S$ , while  $n_C$  stands for the number of components.

**Material balances** in their most general form for an inner column stage can be written as

$$0 = (V_j + S_j^V) \cdot y_{ij} + (L_j + S_j^L) \cdot x_{ij} - V_{j+1} \cdot y_{i,j+1} - L_{j-1} \cdot x_{i,j-1} - F_j \cdot z_{ij},$$

$$i = 1 \dots n_C \quad j = 1 \dots n_S. \quad (4.1)$$

Here the vapour  $F_j^V$  and liquid  $F_j^L$  phase of the feed to the stage  $j$  are considered separately. While this is not strictly necessary it allows for certain freedoms in terms of modelling column operations, as sometimes the vapour fraction of a given feed is actually fed into the vapour phase of a stage and therefore effectively in the liquid phase of the stage above.

A certain amount of the liquid or vapour leaving a stage can be withdrawn from the column by means of the vapour  $S_j^V$  and liquid  $S_j^L$  side draw streams. However it is convenient and seemed to facilitate convergence to define the side draws in terms of dimensionless fractions by relating them to the respective vapour or liquid stream leaving the stage

$$s_j^V = \frac{S_j^V}{V_j}, \quad j = 1 \dots n_S, \quad (4.2)$$

$$s_j^L = \frac{S_j^L}{L_j}, \quad j = 1 \dots n_S. \quad (4.3)$$

By considering these dimensionless the vapour  $s_j^V$  and liquid  $s_j^L$  side draws the material balance can be rewritten as

$$0 = (1 + s_j^V) \cdot V_j \cdot y_{ij} + (1 + s_j^L) \cdot L_j \cdot x_{ij} - V_{j+1} \cdot y_{i,j+1} - L_{j-1} \cdot x_{i,j-1} - F_j \cdot z_{ij},$$

$$i = 1 \dots n_C \quad j = 1 \dots n_S. \quad (4.4)$$

As the model is also to be used for optimization purposes further extensions are necessary. The location of individual feeds as well as the number of theoretical or real stages of the column is to be optimized. To accommodate that need, new variables are needed, namely the feed split  $\zeta_{ij}^F$  for feed  $i$  to stage  $j$  as employed by [9] are introduced. The split variables are integer variables that can take a value of either 0 or 1. Additionally it is assumed that each feed will only be fed to a single stage thus

$$1 = \sum_{j=1}^N \zeta_{ij}, \quad i = 1 \dots n_F, \quad j = 1 \dots n_S, \quad (4.5)$$

where  $n_F$  denotes the number of feeds.

In order to optimize the number of stages several superstructures are possible. One can optimize the reboiler reflux location and condenser reflux location or each single one along with the feed and side

draw locations. The stage number is then changed as all stages between condenser or reboiler reflux are effectively rendered inactive. The solution of the mass and energy balances for each respective stages becomes trivial as only one single vapour or liquid stream enters and exits the stage. While the choice if condenser and or reboiler reflux is optimized is somewhat arbitrary some studies have shown [12] that the strategy of optimizing only feed location and reboiler reflux location possesses some numerical advantages in terms of performance of the solution algorithm.

With the newly introduced split variables for liquid  $\zeta_{ij}^L$  and vapour  $\zeta_{ij}^V$  as well as the reboiler reflux  $\zeta_j^R$  and the liquid  $\zeta_{ij}^{SL}$  and vapour  $\zeta_{ij}^{SV}$  side draws, the material balances can be written as

$$0 = (1 + s_j^V) \cdot V_j \cdot y_{i,j} + (1 + s_j^L) \cdot L_j \cdot x_{i,j} - V_{j+1} \cdot y_{i,j+1} - L_{j-1} \cdot x_{i,j-1} - \sum_{k=1}^{n_F} \zeta_{kj} \cdot F_j \cdot z_{i,j} - \zeta_j^R \cdot V_{n_S} \cdot y_{i,n_S},$$

$$i = 1 \dots C, \quad j = 1 \dots n_S, \quad k = 1 \dots n_F. \quad (4.6)$$

Furthermore to be able to optimize side draws, the stripping factors have to be reformulated accordingly

$$s_j^V = \frac{\sum_{i=1}^{n_{SV}} \zeta_{ij}^{SV} S_j^V}{V_j}, \quad j = 1 \dots n_S, \quad i = 1 \dots n_{SV}, \quad (4.7)$$

$$s_j^L = \frac{\sum_{i=1}^{n_{SL}} \zeta_{ij}^{SL} S_j^L}{L_j}, \quad j = 1 \dots n_S, \quad i = 1 \dots n_{SL}. \quad (4.8)$$

**Equilibrium** between a vapour and liquid phase is achieved when the chemical potentials for each component in the phases are equal. This is commonly expressed by an equilibrium  $K_i$  constant. With that the equilibrium equation can be written as

$$y_i^{eq} = K_i \cdot x_i, \quad i = 1 \dots n_C. \quad (4.9)$$

The requirement for equal chemical potentials can be expressed in terms of the vapour  $f_i^V$  and liquid  $f_i^L$  fugacities [2].

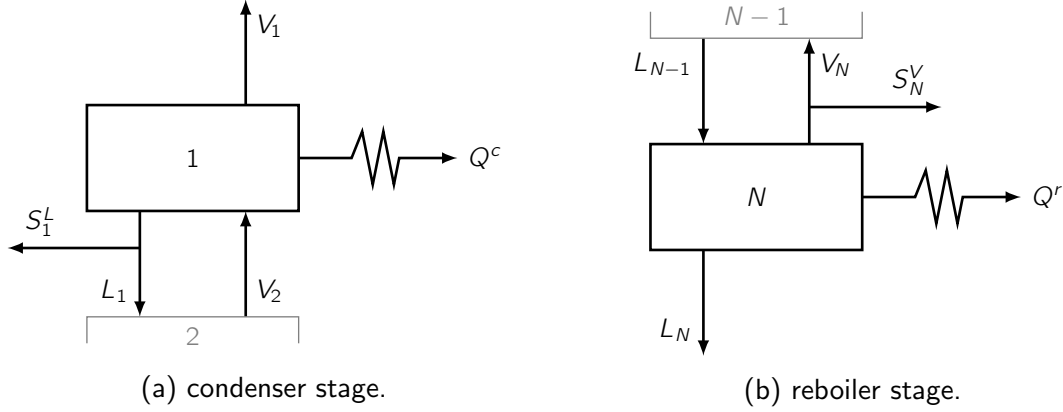
$$f_i^V = f_i^L, \quad i = 1 \dots n_C. \quad (4.10)$$

This can also be written in terms of the liquid activity coefficient  $\gamma_i$ , the pointing factor  $F_{Pi}$ , the reference vapour fugacity coefficient  $\varphi_i$ , the vapour pressure  $p_i^S$  as well as the system pressure  $p$  along with the vapour and liquid molar fractions

$$\gamma_i F_{Pi} \varphi_i^0 p_i^S x_i = \varphi_i p y_i, \quad i = 1 \dots n_C. \quad (4.11)$$

By reformulating eq. (4.12) an expression for the equilibrium ratios can be derived

$$y_i^{eq} = \underbrace{\frac{\gamma_i F_{Pi} \varphi_i^0 p_i^S}{\varphi_i p}}_{K_i} x_i, \quad i = 1 \dots n_C. \quad (4.12)$$



The equations to determine the quantities used when computing the equilibrium ratios are by themselves functions of temperature, pressure, and vapour as well as liquid molar fractions. They are further discussed in sec. ?? . It therefore becomes evident that the equilibrium ratios are a major source non-linearities in the MESH equations.

When simulating a distillation process one might consider only equilibrium stages. This however will in most cases not reflect the true behaviour of a given stage as the time a vapour and liquid phase are in contact might not be sufficient to achieve equilibrium. This can be accounted for by introducing the Murphee tray efficiency [14]

$$\eta_{ij}^{eq} = \frac{y_{ij} - y_{ij+1}}{y_{ij}^{eq} - y_{ij+1}} \quad i = 1 \dots n_C \quad j = 1 \dots n_S. \quad (4.13)$$

While several models to approximate these efficiencies have been investigated, their predictions are most often rather poor [8] and their evaluation rather complex. Furthermore as indicated in the formula they might differ for different species involved. For the scope of this model however they are not computed separately, but rather supplied and assumes uniform for each stage and component.

**Enthalpy balances** are again written considering the previously defined stripping factors and splitting variables

$$\begin{aligned} 0 = & (1 + s_j^V) \cdot V_j \cdot h_j^V + (1 + s_j^L) \cdot L_j \cdot h_j^L - V_{j+1} \cdot h_{j+1}^V \\ & - L_{j-1} \cdot h_{j-1}^L - \sum_{k=1}^{n_F} \zeta_{kj} \cdot F_k \cdot h_j^F - \zeta_j^R \cdot V_N \cdot h_N^V, \\ & i = 1 \dots C, \quad j = 1 \dots N, \quad k = 1 \dots n_F. \end{aligned} \quad (4.14)$$

**Condenser and reboiler** are modeled more or less as regular column stages. However they possess certain specialties that are explicitly considered in the column model. For one it is assumed that no feeds enter the reboiler and condenser stage. Furthermore no vapour side stream is drawn from the condenser stage and no liquid side stream from the reboiler stage.

Additionally the condenser stage needs to be examined a little further. In terms of operations several assumptions can be made for the condenser. In general one can distinguish a total, partial vapour and partial vapour liquid condenser. For the total condenser all vapour that enters the respective stage is condensed and only liquid product is drawn. The partial vapour condenser condenses only the vapour that is fed back into the column and all product that is drawn is gaseous. The partial vapour liquid condenser denotes the most general case, where part of the incoming vapour is condensed and product is drawn from the vapour and liquid phase. The most important thing to consider in these different cases, is that while in both partial condensers a vapour liquid equilibrium takes place, due to the absence of vapour the same does not hold for the total condenser. To accommodate that fact the MESH equations have to be adjusted [19]. While the material and energy balances remain unchanged the equilibrium equations have to be altered. First the vapour and liquid compositions are set equal for all but one component

$$x_{i1} = y_{i1} \quad i = 1 \dots C - 1, \quad (4.15)$$

and the condenser temperature is determined by the bubble point equation

$$1 = \sum_i K_{i1}(T_1, p_1, x_1, y_1) \cdot x_{i1} \quad i = 1 \dots n_C. \quad (4.16)$$

When implementing the model in a process simulator it is sensible to consider, that due to the limited accuracy of computers the omitted component in eq. (4.15) needs to be a non-trace component in the condenser stage. The implemented model therefore has to specify such a component when a total condenser is chosen to avoid numerical difficulties.

In practice it is highly unlikely, that the exact amount of energy required to condensate all liquid will be drawn from the condenser. More likely, if all vapour is condensed, a little more energy will be withdrawn and slightly sub-cooled liquid will leave the condenser. Therefore the model includes the possibility to specify a degree of sub-cooling  $T^{sub}$  which will be considered when calculating bubble point temperature

$$1 = \sum_i K_{i1}(T_1 + T^{sub}, p_1, x_1, y_1) \cdot x_{i1} \quad i = 1 \dots n_C. \quad (4.17)$$

**Pressure** along the entire column is often specified in the steady-state case. However as it is inconvenient and unpractical to specify a pressure for each stage one might either specify a pressure at the top and bottom stage and assume a uniform pressure profile along the column, or specify either top  $p_1$  or bottom pressure  $p_N$  along with a total pressure drop  $\Delta p$ , or a stage-wise one  $\Delta p_{stage}$ . However the issue is further complicated if one considers the case of optimization for number of trays. In that case several trays will become inactive. For those trays the mass and energy balances become trivial, as only liquid enters and exits these trays. (For the case employed here, where the reboiler reflux is being optimized). This also means, that from the last active tray down to the reboiler – if present – there should be a uniform profile. However, if a uniform pressure profile from that stage down is not enforced, the solver will have to compensate for slight changes in the equilibrium due to pressure variations with minimal vapour flow-rates. This is very undesirable, as it might lead to

severe problems in the solver, or the calculation of other properties, dependent on these values. To account for this issue, the reboiler reflux split can once more be employed

$$p_i = p_{j-1} + \left(1 - \sum_{k=1}^{j-1} \zeta_k^R\right) \cdot \Delta p_{j-1} \quad j = 1 \dots n_S. \quad (4.18)$$

As an alternative to specifying the pressure, one might consider calculating the pressure drop from (semi)-empirical models. There are numerous correlations for different types of column internals. These correlations become particularly important if column dynamics are to be considered, as they make a connection between holdups and flow-rates within the column. Two different pressure drop models have been implemented, one for trayed columns and another one for structured packings. As they are closely tied to dynamics, they will be discussed in closed detail in sec. ??.

## Specifications & initialization

The equation systems presented above is comprised of  $NC$  component balances,  $NC$  equilibrium equations,  $2N$  summation equations and  $N$  energy balances. This gives a total of  $N(2C + 3)$  equations. On the other hand there are  $N$  temperatures and pressures,  $2N$  molar flow rates,  $N$  energy streams, and  $NC$  vapour as well as liquid concentrations. Additionally the feed flow rates compositions and temperatures and the side draw split fractions or flow rates appear as variables. The feeds and side draws would usually be specified, which leaves a total of  $N(2C + 5)$  variables.

The pressure profile of a distillation column is usually specified. Either by explicitly assigning a given pressure to each stage, or more conveniently by defining a pressure either the top or bottom pressure as well as the pressure drop per stage

$$\Delta p_{stage} = p_i - p_{i-1}, \quad i = 2 \dots N. \quad (4.19)$$

In terms of unit operations this pressure drop is of high significance, as many columns can only be feasibly operated, if the pressure drop does not exceed certain limits. In case of the ASU the production of Argon only became feasible as structured packings, which display a very low pressure drop, became available. This is due to the large number of theoretical stages required to attain the desired Argon purities.

The energies  $Q_i$  denote addition heaters or cooler on the respective stages. For all intermediate stages these values would be specified as well. If all energies would be specified, that would – along with the pressure profile – sum up to  $2N$  specifications, which leaves  $N(2C + 3)$  unknowns. As the number of equations and unknowns are the equal, this system can then be solved.

In practice it is often challenging to correctly guess the condenser and reboiler heat loads in advance. This is especially true since they have a tremendous impact on the overall performance of the column. Hence it is often desirable to supply other specifications than the respective heat loads. To allow for such specification so called discrepancy functions can be introduced [14], which replace the energy balance for the condenser and / or reboiler stage.

One common specification is the so called reflux ratio  $\nu^D = \frac{L_1}{V_1 + S_1^L}$  for the condenser, or the boilup ratio  $\nu^R = \frac{L_N}{V_N}$  for the reboiler. They are defined as the ratio of the molar flowrate sent back into the

section  
super-  
fluous?  
init  
proced-  
ure de-  
scriben  
in impl  
sec...

| specification              | replacement for $H_1$                 | replacement for $H_N$        |
|----------------------------|---------------------------------------|------------------------------|
| reflux or boilup ratio     | $0 = L_1 - \nu^D \cdot (V_1 + S_1^L)$ | $0 = V_N - \nu^R \cdot L_N$  |
| temperature                | $0 = T_1 - T_{spec}$                  | $0 = T_N - T_{spec}$         |
| product flowrate           | $0 = (V_1 + S_1^L) - D$               | $0 = L_N - B$                |
| component product flowrate |                                       | $0 = L_N \cdot x_{iN} - b_i$ |
| mole fraction              | $0 = y_{i1} - y_{i,spec}$             | $0 = x_{iN} - x_{i,spec}$    |

Table 4.1: discrepancy functions for different column specifications.

column over the product flowrate which leaves the column. For the reboiler this denotes a liquid stream, while for the condenser the product can be gaseous and liquid. Specifying this leads to

$$0 = L_1 - \nu^D \cdot (V_1 + S_1^L), \quad (4.20)$$

$$0 = V_N - \nu^R \cdot L_N, \quad (4.21)$$

as discrepancy functions. In addition to that further specifications are conceivable. Most commonly distillate ( $D$ ) or bottoms ( $B$ ) flow rates, or purities, component flow rates ( $d_i$ ,  $b_i$ ) or temperatures. The corresponding discrepancy functions are summarized in tab. 4.1.

The specifications for the reboiler stage are quite straightforward, in contrast to that, different cases for the condenser have to be considered. In the most general case the top product can be drawn as vapour and liquid. This case is here called a partial vapour liquid condenser. The other cases are a total condenser, where all the vapour entering the condenser stage is condensed, and all product is drawn as a liquid stream, as well as a partial vapour condenser, where only the reflux is condensed and all product is drawn as vapour. As discussed earlier no VLE takes place in the condenser stage, if a total condenser is specified, which needs to be accounted for. Both the total and partial vapour condensed implicitly include an extra specification since in former case the top vapour product flow rate becomes zero and in the latter the top liquid product flowrate. Furthermore a specification of the condenser energy is infeasible as well as implicitly given for the total condenser. In case of the partial vapour liquid condenser no implicit specification is given, which requires an additional specification. In general two top specifications are necessary, whereas only one bottom specification is required. These top specification can include the condenser duty, any top flowrate, the reflux ratio as well as a newly introduced quantity, the top vapour fraction defined as

$$\nu^{vap} = \frac{V_1}{V_1 + S_1^L}. \quad (4.22)$$

As mentioned before the solution of the MESH equations can pose a considerable problem to numerical solvers. It is therefore necessary to supply the solver with feasible estimates for the involved variables that can be used as an initial guess for convergence of the process model. A lot of effort has been spent to formulate robust strategies to initialize distillation column models. One of the most prominent is the so called Inside-Out algorithm first introduced by Boston and Sullivan [5]. Within this algorithm an inner and outer iterative loop are employed. Within the outer loop approximate parameters for simplified models of phase equilibrium and enthalpy are computed by rigorous thermodynamic models and guesses for stage temperatures and concentrations. Within the inner loop new stage temperatures and concentrations are attained by solving the MESH equations using the simplified thermodynamic models. Once the inner loop converges the simplified model parameters are updated within the outer loop by means of the newly calculated temperatures and



concentrations. This algorithm converges in many cases even for very poor initial guesses and has been extended to handle complex columns with side-draws and even reactive distillation [4]. It is still in use in the process simulator Aspen Plus<sup>®</sup>. However as it is used within an modular algorithmic environment it is not applicable to equation based simulators such as gPROMS<sup>®</sup>.

More recently other approaches have been published to attain improved initial guesses. Fletcher and Morton [11] proposed the solution of a column model at infinite reflux and zero feed flow rate. This leads to a much simplified model which can be solved more easily. The computed purities and stage numbers can give valuable insight into the process model. As this approach relies on the solution of a simplified model and has no algorithmic elements, it can be implemented in equation based process simulators.

Another strategy that has been successfully applied to zeotropic and azeotropic mixtures relies on solving the column model for the limiting case of the adiabatic column [3]. The adiabatic column in this case is the column with the minimal entropy production in a real column. To avoid entropy production all streams that come in contact must be in equilibrium. To achieve this the column would have to employ an infinite number of stages and have an infinite number of heat exchangers along its length. The adiabatic column then uses only two heat exchanger in the condenser and reboiler stage and assumes a pinch point at the feed stage.

Furthermore a much simpler approach has proven adequate for many applications [14] which is also employed as a starting point in this work. Therein feed properties are used as initial guesses. First a linear temperature profile from the boiling temperature to dew temperature of the combined feed mixture is used to initialize temperatures, whereas a simple flash at average column pressure and feed temperature yields a vapour and liquid concentration which is used as uniform profile for every column stage. However as the feed might be sub-cooled liquid or super-heated vapour, the TP-Flash is replaced by a specified vapour fraction. As vapour fraction for the flash initial estimates of the vapour and liquid flow rates at the top and bottom of the column are used. The stage-wise molar flow-rates are computed from the constant molal overflow assumption, which postulates a constant heat of vaporization and yields therefore uniform liquid and vapour flow-rates within a column section. A section in this case is denoted by any feed location where the flow-rates change due to the added feed. In the feed stages a super heated or sub-cooled feed is also considered by means of an extended vapour fraction

$$q^F = \frac{h^F - h^L}{h^V - h^L}. \quad (4.23)$$

While this approach leads to model convergence in many cases, it is not entirely robust. While the system considered in this case displays only moderate non-idealities it is highly cupeled. Especially the low pressure column (LPC) has multiple feeds and side draws, which leads to non-convergence if the aforementioned initialization strategy is employed. However the fact that the system is not highly non-ideal can be exploited. Whenever the K-values are not too much dependent on mixture composition an intermediate step can be used to refine concentration guesses. The constant molal overflow assumption is retained and the equilibrium ratios are computed based on the initial guesses from the first stage. The component balance is then reformulated only in terms of liquid component

elaborat  
on adia-  
batic  
column

flow-rates  $l_{ij}$

$$0 = \left( (1 + s_j^V) \cdot K_{ij} \cdot \frac{V_j}{L_j} + (1 + s_j^L) \right) \cdot l_{ij} - \frac{V_{j+1}}{L_{j+1}} \cdot K_{ij+1} \cdot l_{ij+1} - l_{ij-1} - F_j^V \cdot z_{ij}^V - F_j^L \cdot z_{ij}^L, \quad i = 1 \dots n_C \quad j = 1 \dots n_S. \quad (4.24)$$

eq. (4.24) is linear in the liquid component flow rates. Furthermore vapour component flow rates are substituted in the linear component balance and can be computed by

$$v_{ij} = K_{ij} \cdot \frac{V_j}{L_j} \cdot l_{ij} \quad i = 1 \dots n_C \quad j = 1 \dots n_S. \quad (4.25)$$

On of the reasons eq. (4.24) is formulated in terms of component flow rates rather than molar fractions, is that the molar fraction computed in that manner would not be normalized. If the mole fractions are computed from the component flow rates normalization is implicitly given

$$x_{ij} = \frac{l_{ij}}{\sum_k^C l_{kj}} \quad i = 1 \dots n_C \quad j = 1 \dots n_S, \quad (4.26)$$

$$y_{ij} = \frac{v_{ij}}{\sum_k^C v_{kj}} \quad i = 1 \dots n_C \quad j = 1 \dots n_S. \quad (4.27)$$

The total molar flow rates used in eq. (4.24) are computed by solving stage-wise total mass balances under the constant molal overflow assumption. This assumption postulates that the heat of vaporization is independent of system composition. Therefore always the same amount of liquid enters and leaves a given stage

$$0 = L_j + S_j^L - L_{j-1} - (1 + q_F^L) \cdot F_j^L - q_F^V \cdot F_j^V \quad j = 1 \dots N. \quad (4.28)$$

Only at feed and side draw stages the total flow rates change. To introduce some more accuracy to the model, the available information about the feed is considered. When a feed enters as super-heated vapour or sub-cooled liquid, it has the capability to evaporate some liquid or liquefy some vapour. To account for that fact the feed energy parameters  $q_F^L$  and  $q_F^V$  are introduced

$$q_i^{FV} = \frac{H_i^{FV} - H_i^V}{H_i^V - H_i^L}, \quad i = 1 \dots F^V, \quad (4.29)$$

$$q_i^{FL} = \frac{H_i^{FL} - H_i^L}{H_i^V - H_i^L}, \quad i = 1 \dots F^L. \quad (4.30)$$

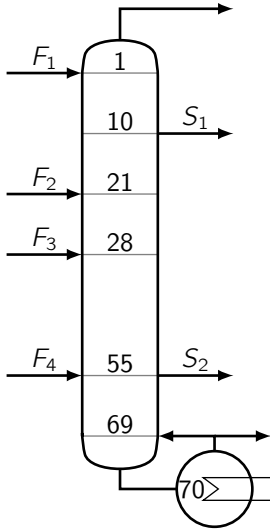
The vapour total flow rates are then computed from the total mass balances

$$0 = L_j + S_j^L + V_j + S_j^V - L_{j+1} - V_{j+1} - F_j^L - F_j^V, \quad j = 1 \dots N. \quad (4.31)$$

As no energy balances are included at this stage, the condenser and reboiler stage are characterized by the reflux ( $\nu^c = \frac{V_1}{L_1}$ ) or boilup ratio ( $\nu^r = \frac{V_N}{L_N}$ ) respectively. This leads to

$$0 = V_1 - \nu^c \cdot L_1, \quad (4.32)$$

$$0 = L_N - \nu^r \cdot V_N. \quad (4.33)$$



| feed specifications |                            |               |               |              |         |           |
|---------------------|----------------------------|---------------|---------------|--------------|---------|-----------|
| stream              | flow [ $\frac{kmol}{hr}$ ] | $z_{O_2} [-]$ | $z_{N_2} [-]$ | $z_{Ar} [-]$ | $T [K]$ | $p [bar]$ |
| $F_1$               | 2985.77                    | 4.674E-10     | 0.9999        | 6.378E-7     | 79.45   | 1.3       |
| $F_2$               | 1836.36                    | 0.2095        | 0.7812        | 0.0093       | 98.91   | 1.3       |
| $F_3$               | 7609.06                    | 0.2920        | 0.6950        | 0.0130       | 81.88   | 1.3       |
| $F_4$               | 774.94                     | 0.9161        | 5.393E-12     | 8.394E-2     | 92.13   | 1.8       |

| column specifications |            |            |              |           |           |
|-----------------------|------------|------------|--------------|-----------|-----------|
| stages                | $S_1$ frac | $S_2$ frac | boilup ratio | $p^{top}$ | $p^{bot}$ |
| 70                    | 10         | 0.15       | 3.5          | 1.2 bar   | 1.3 bar   |

Table 4.2: column specifications.

Figure 4.3: example column.

To close the equation system the global mass balance is included

$$0 = V_1 + L_N + \sum_{j=1}^N (S_j^V + S_j^L - F_j^V - F_j^L), \quad j = 1 \dots N. \quad (4.34)$$

For more complex systems more elaborate strategies have been developed, which essentially try to incorporate some of the principals from the inside out algorithm into an equation based environment. The process simulator gPROMS<sup>®</sup> allows for definition of standardized initialization procedures as well as different model variants that can be solved consecutively. With that strategies were developed that proved successful for more complex mixtures and even three phase systems. As these strategies are closely linked to the implementation in gPROMS<sup>®</sup> and the programm capabilities, they will be discussed in sec. 4.5

Furthermore it should be noted, that not all specifications are compatible with the initialization strategies described above. While this issue has been addressed, it also will be explained in the implementation section.

**Example** To illustrate how the initialization procedure works an example has been constructed of a rather complex column – or column section – with multiple feeds and side draws (fig. 4.2). It is taken from an example process of cryogenic air separation. The column in question is a column section without an condenser stage and displayed the most difficulties in terms of convergence when constructing the process flowsheet.

In addition to the aforementioned initialization strategy, columns with side draws present are handled in a slightly different manner. Initially the side draws are disregarded. Then the initialization procedure is carried out. Once the column without side draws has converged, a homotopy approach

$$f(\mathbf{x}) = (1 - \alpha) \cdot f_0(\mathbf{x}) + \alpha \cdot f_1(\mathbf{x}) \quad (4.35)$$

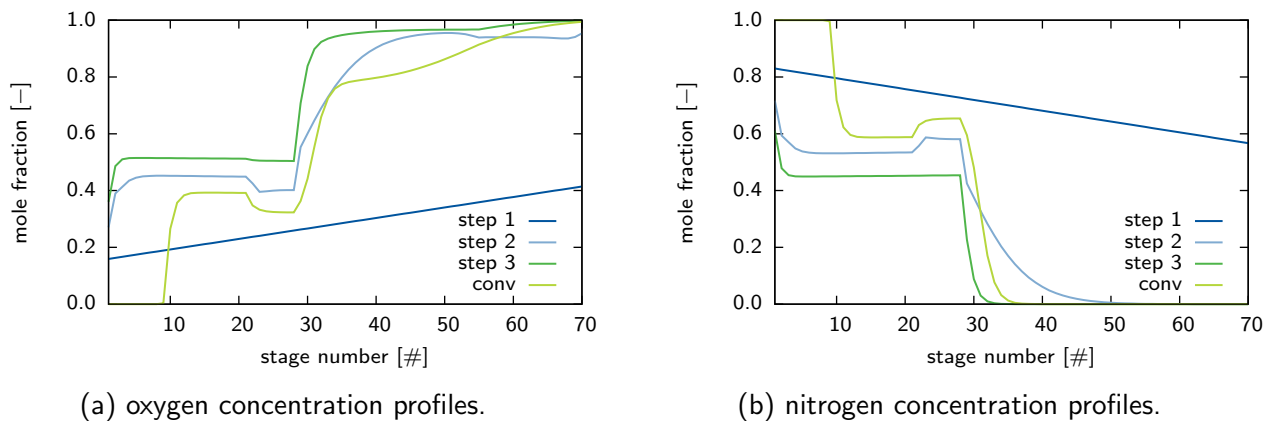


Figure 4.4: initialization example concentration profiles.

is employed, where the parameter  $\alpha$  is initially set to zero and then gradually moved to a value of one. During the initialization homotopies could generally be employed to move from one step to another. While in some cases robustness is improved by such a strategy, it is always computationally far more expensive than simply jumping between different stages.

For clarity reasons the different steps of the initialization procedure are repeated in a tabular manner

1.
  - linear temperature profile between dew ( $T^{dew}$ ) and bubble point temperature ( $T^{bub}$ ) of mixed feed.
  - linear profile between feed flash vapour and liquid compositions for liquid stage compositions.
  - constant profile for vapour compositions.
  - molar flow rates from constant molar overflow model.
  - side draw flow rates set to zero.
2.
  - total molar flow rates from constant molar overflow model.
  - simplified equilibrium ratios from initial liquid mole fractions and linear temperature profile.
  - liquid and vapour mole fractions from linearized mass balances.
3. rigorous solution of MESH equations with side draws still set to zero.
4. homotopic approach to MESH equations with side draws considered.

The resulting profiles for oxygen and nitrogen concentrations in the example column can be seen in fig. 4.4a and fig. 4.4b.

### 4.1.2 Integrated condenser & reboiler

The integrated condenser reboiler unit can be considered as the most influential unit regarding operations and simulation of the double effect column. This stems from the fact, that each change in the parameters and operation of this unit will reverberate through the entire process, as they will simultaneously affect boil-up ratio and reflux ratio of the column, both major operational parameters

mention  
prob-  
lems  
and  
bounded  
homo-  
topy?

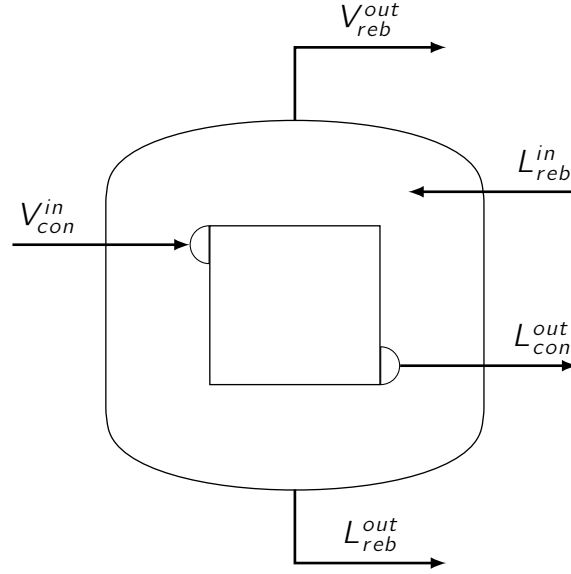


Figure 4.5: Integrated condenser & reboiler unit.

with great effect. The strong integration with the material streams between the column sections as well as other side columns does the rest.

Therefore a separate model for this unit was developed, rather than simply establishing a couple between the condenser and the reboiler in the case for two separately modeled column sections.

### Reboiler side

The reboiler side is modeled much like an equilibrium stage in the column, considering the entering and leaving streams as depicted in fig. 4.1.2. However in contrast to the equations supplied for the column, no integer optimization terms will have to be considered. Furthermore no side draws, or separate feeds are recognized. With that the material balances are

$$0 = L_{reb}^{in} x_{i,reb}^{in} - L_{reb}^{out} x_i^{reb} - V_{reb}^{out} y_i^{reb}, \quad i = 1 \dots n_C. \quad (4.36)$$

The energy balance taking into account the transferred energy ( $Q_{CR}$ ) becomes therefore

$$0 = L_{reb}^{in} h_{reb}^{in} - L_{reb}^{out} h_{reb}^L - V_{reb}^{out} h_{reb}^V + Q_{CR}. \quad (4.37)$$

The equilibrium and summation equations are analogous to the ones presented for the column model. A pressure drop again is assigned with relation to the lowest column stage.

### Condenser side

The condenser is modeled as a total condenser. The mass and component balances therefore become trivial

$$x_{i,con} = y_{i,con}^{in}, \quad i = 1 \dots n_C, \quad (4.38)$$

$$V_{con}^{in} = L_{con}^{out}. \quad (4.39)$$

The temperature is set to the bubble temperature of the given mixture at an assigned pressure. The enthalpies of the entering and leaving stream can therefore be calculated from the given EOS. And the energy balance determines the transferred energy

$$0 = V_{con}^{in} h_{con}^{in} - L_{con}^{out} h_{con}^L - Q_{CR}. \quad (4.40)$$

### 4.1.3 Heat exchange

The issue of heat integration is essential to the economic performance of cryogenic air separation. Foremost one must consider the special column configuration used in the process. Since operation of the condenser in the low pressure section only becomes possible if the reboiler in the high pressure section functions as heat sink, no external utilities are supplied to either unit. Rather they are combined into a single heat exchange unit. Thus the absolute value of the reboiler energy must be matched by the energy recovered from the condenser. Furthermore the material streams entering the process can – and should – exchange heat with the process streams leaving it. The combined condenser / reboiler for LPC / HPC column is assumed as a given heat exchange. This makes sense insofar, as this is a necessity in terms of the actual physical implementation of the process units. Also the usage of the oxygen rich liquid from the HPC as coolant in the Argon condenser is assumed as fixed.

adjust  
heat ex-  
change  
section  
to cur-  
rent ap-  
proach.

This leaves the process stream leaving the compression stage of the process as well as all product and waste streams leaving the process. All those streams are – for simulation purposes and also in some process implementations – fed into a single multi-stream heat exchange unit. In actual processes all heat exchange and much of the process operations take place in the so called "cold box". As such a heavily insulated area is referred to. This is done to minimize heat exchange with the surroundings. Therefore and for further reasons compact heat exchange units such as plate-fin multi-stream heat exchangers are favoured when dealing with cryogenic processes in general and the cryogenic air separation in particular.

Due to the importance of heat integration to the ASU process some thought should be given as to what modelling approach should be employed. Although the field of heat integration is one of the most intensively studied within process engineering, only a limited amount of approaches is available in open literature [15].

Traditionally heat integration has been carried out in a sequential manner, where it is for the purposes of process optimization assumed, that all heating and cooling is done by external utilities. After an (locally) optimal process configuration is identified, all hot and cold streams within the process are identified, and their temperature intervals fixed. In subsequent steps first the minimum utility requirements, and maximum number of heat exchangers are identified, and a specific heat exchange network (HEN) is designed. While this approach has been successfully applied to a multitude of processes and led to substantial savings, it is questionable if such a sequential approach will yield an optimal or near optimal solution.

add  
citation  
Lind-  
hoff...

Therefore some efforts have been made to develop efficient strategies for simultaneous process optimization and heat integration. Two general approaches can be distinguished. The first one based on the pinch concept.

elaborate on pinch concept?

These methods are able to identify the minimum heat requirement as well as stream temperatures during process optimization. The first model along these lines was published by Duran and Grossmann [10] in 1986. They introduced a limited number of quite well behaved constraints into the optimization model to ensure no minimum driving force violations. Recently this model has been extended to handle phase changes and by fixing the utilities to zero been applied to the design of a multi-stream heat exchanger [15]. The major drawback with these methods

read about and mention transshipment model by Moriari (sequential)

is that one cannot target area of a given heat exchanger as the approach temperatures are not computed by the model. Therefore the sometimes substantial trade-off between the cost for heat exchange area and utility cost cannot be regarded.

A second approach employs superstructures of a HEN to find optimal matchings of process streams. No pinch point calculations are required, as the actual heat exchange is more or less modeled explicitly. This leads to the benefit, that approach temperatures as well as exchanged heat duties between each stream coupling are known within the model, and the cost of the designed unit can be considered in an economic objective function.

The approach and respective superstructure adapted in this thesis were first published by Yee and Grossmann [26]. Fig. 4.6 shows the stage wise superstructure for a HEN consisting of two hot and two cold streams.

In this stagewise structure each hot stream can exchange heat with each cold stream within each stage. The following assumptions were made when the model was developed

- Constant heat capacities
- Constant heat transfer coefficients
- Countercurrent heat exchangers
- Isothermal mixing at each stage.

The assumption of constant heat capacities is a common one in the design of HEN's. When no phase boundaries are passed and the temperature range of the involved is not too wide, it is a reasonably good approximation of the real conditions. While constant heat transfer coefficients are assumed the model leaves the flexibility to define different coefficients for each pairing of hot and cold streams. Countercurrent heat exchangers are common in industrial practice. This assumption however does not really pose a limitation, as the model can easily be altered to account for concurrent units.

The last assumption of isothermal mixing is a more major one. It has been introduced as it allows for significant simplifications and leads to a model, where all constraints are linear and all non-linearities are restricted to the objective function. While that is certainly not true for the entire process model, it should at least allow for some reductions in the model complexity. The assumption states, that regardless of which streams a given stream exchanges heat with, it will leave at the same temperature. Due to that all energy balances around each unit in the superstructure can be eliminated as well as the subsequent mixing of the streams.

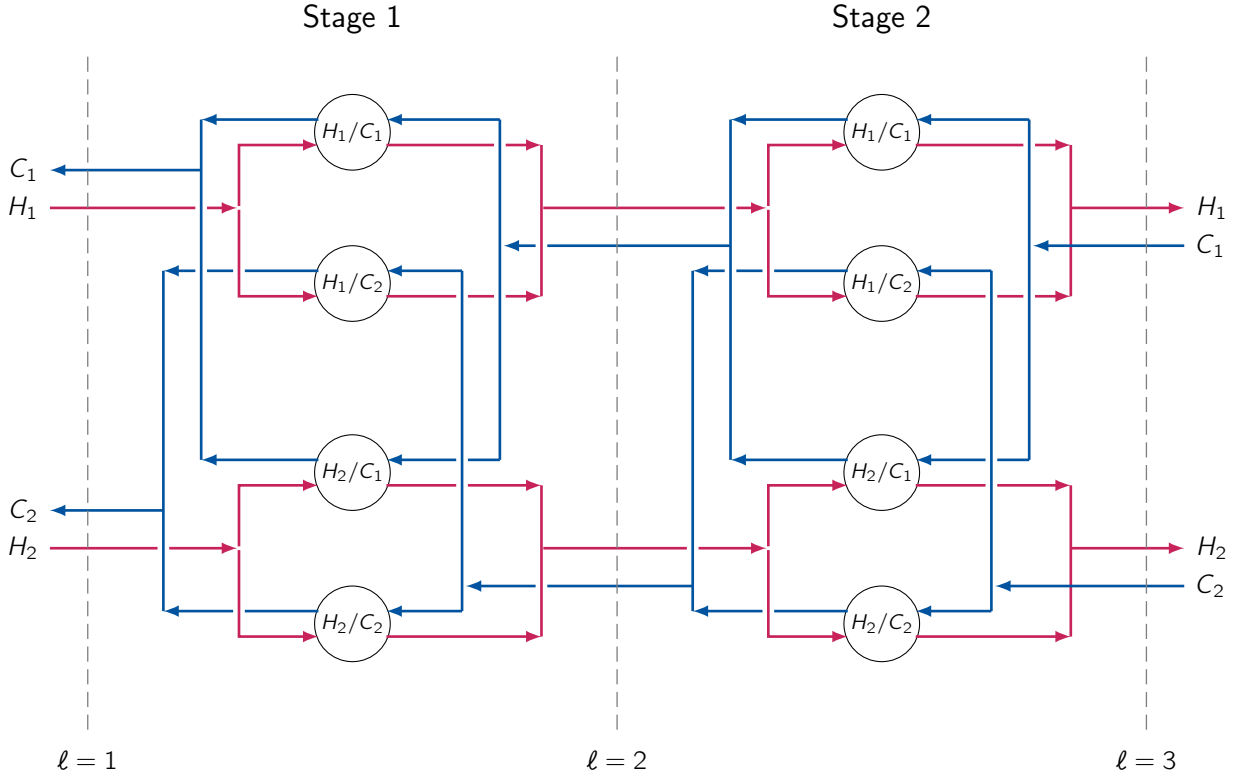


Figure 4.6: Superstructure for multi-stream heat exchanger. [26]

**Model equations** First of all a heat balance at each stage is necessary

$$F_i(T_{i,\ell} - T_{i,\ell+1}) = \sum_j q_{ijk} \quad (4.41)$$

$$f_j(T_{i,\ell} - T_{i,\ell+1}) = \sum_i q_{ijk} \quad (4.42)$$

The heat exchange area  $A_{hx}$  can be computed from the exchanged energy, the heat transfer coefficients  $\alpha_{ij}$  and the logarithmic mean temperature difference  $LMTD$ .

$$A_{hx} = \sum_i \sum_j \sum_k \frac{q_{ijk}}{\alpha_{ij} * LMTD_{ijk} + \delta} \quad (4.43)$$

While the small number  $\delta$  is included to avoid problems in the program, when  $LMTD$  becomes zero. In order to avoid further numerical difficulties when the approach temperatures  $\Delta T_{ij}$  at each side of an exchange unit approach zero, it was proposed to use an approximation introduced by Chen [7]

$$LMTD_{ijk} \approx \left[ \Delta T_{ijk} \cdot \Delta T_{ijk+1} \frac{\Delta T_{ijk} + \Delta T_{ijk+1}}{2} \right]^{\frac{1}{3}}. \quad (4.44)$$

While the approach temperatures are defined as

$$\Delta T_{ijk} = \max \{0, T_{ik} - T_{jk}\} \quad (4.45)$$

AS the max function is non-smooth and thus non differentiable at the points  $T_{ik} = T_{jk}$ , gPROMS<sup>®</sup> internally uses a smooth approximation. The exact form of which is unknown to the author.



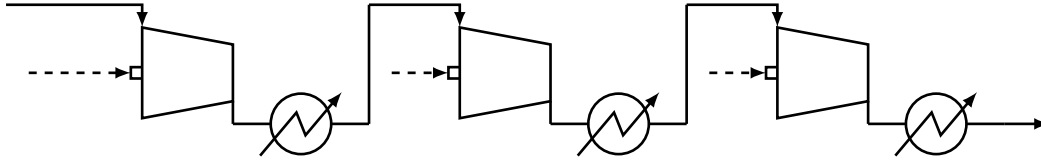


Figure 4.7: Multi-stage compression.

#### 4.1.4 Compression & expansion

The issue of cooling the ambient air to process temperatures at around 90K is not an easy one. The main hindrance is, that a heat sink at this temperature level is not readily available. Lucky thermodynamics offer a different way to reach such temperatures. In order to do so, the ambient air first needs to be compressed and then expanded again. Cooling then occurs by either exploiting the *Joule-Thompson* effect or isentropic expansion. First a few comments are made about the compression stage, while afterwards the governing principles for cooling by expansion will be described.

##### Multi-stage compression

Compressors and expanders are among the most common process equipment. A multitude of processes utilizes them as primary or auxiliary units. In the context of cryogenic air separation the compression plays a major role, as it enables to reach temperatures needed for liquefying air and gases in general. As the compression of gases is always associated with a significant reduction in volume it requires large amounts of energy. Thus in addition to significantly contributing to the capital cost of the process the compression stage is responsible for the majority of the operating cost encountered in the ASU process.

The rigorous modeling of continuous flow machines in terms of unit operations poses great challenges. For specific units it may be undertaken by means of CFD simulations or employing characteristics diagrams, which require extensive experiments and can usually be obtained from the manufacturer. For the purposes of process design however a simpler approach with unit efficiencies is appropriate.

As a significant temperature increase goes along with the compression of air and in order to reduce the energy demand of the compression in general, it is beneficial, to use a multi stage compressor with inter-cooling as depicted in fig. 4.7. This yields a lower energy consumption as a single stage unit for the same compression ratio.

Subsequently the working equations for the compressor model used in the scope of this thesis are briefly summarized.

A trivial material and component balance around the compressor yields the outlet molar flow-rate  $F^{out}$  as well as the outlet overall composition  $z^{out}$

$$0 = F^{in} - F^{out}, \quad (4.46)$$

$$0 = z_i^{in} - z_i^{out} \quad i = 1 \dots n_C. \quad (4.47)$$

revise  
com-  
pressor  
equa-  
tions  
and  
add  
equa-  
tions to  
nomen-  
clature

To calculate the mechanical work associated with the desired compression, first the isentropic case

$$S^{in} = S^{out} \quad (4.48)$$

is considered.

$$W_S = F^{in} \cdot (H^{in} - H^{out}) \quad (4.49)$$

$$W \cdot \eta^C = W_S \quad (4.50)$$

$$W_S = F^{in} \cdot H^{in}(T^{in}, p^{in}, z_i^{in}) - F^{out} \cdot H^{out}(T^{out}, p^{out}, z_i^{out}) \quad (4.51)$$

### Pressure drop

$$p^{out} = p^{in} + \Delta p \quad (4.52)$$

### Cooling by expansion

The liquefaction of gases requires temperatures well below ambient conditions. In order to reach such conditions one cannot utilize natural occurring coolants, but rather cooling effects that occur during the expansion of compressed gases. First we consider the expansion through an expansion valve or so called *Joule-Thompson* - valve. If we assume very good insulation of conditions this expansion can closely be approximated by an isenthalpic process ( $h_1 = h_2$ ). To describe the change in temperature during isenthalpic expansion the *Joule-Thompson* coefficient

$$\mu_{JT} = \left( \frac{\partial T}{\partial p} \right)_h, \quad (4.53)$$

which denotes pressure derivative of the temperature at constant enthalpy can be considered. This can be transformed into

$$\mu_{JT} = \frac{1}{c_p} \left[ T \left( \frac{\partial v}{\partial T} \right)_p - v \right] \quad (4.54)$$

If we employ the Peng-Robinson equation of state we can plot the isenthalpes for ambient air ( $x_{N_2} = 0.7812$ ,  $x_{O_2} = 0.2095$ ,  $x_{Ar} = 0.0093$ ) in a PT-diagramm (fig. 4.8). One can easily see, that in certain ranges a pressure decrease will result in an increase in temperature, while for other regions in a decrease. It is interesting to mention that the non-idealities of a given gas give rise to this effect. For an ideal gas the temperature change at isenthalpic expansion would always be zero. Luckily for the cryogenic engineer real gases deviate from ideal behaviour especially at elevated pressures and low temperatures. It is therefore important to give some consideration to the thermodynamic model

elaborat  
on dif-  
ferent  
terms.

add de-  
rivative  
in ap-  
pendix?

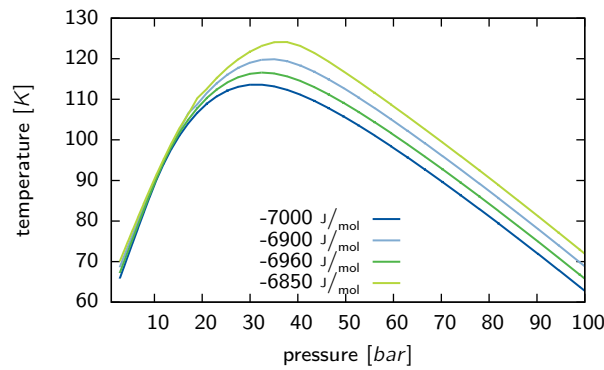


Figure 4.8: Isenthalpes computed by Peng-Robinson EOS.

used to describe the properties of the system in question, as the non-ideal properties need to be captured appropriately.

A different way of expanding a compressed gas, is by letting it produce work in an fluid kinetic machine. If one assumes an adiabatic devices and disregards irreversible effects, this process can be viewed as isentropic. Analogous to the isenthalpic case an isentropic expansion coefficient can be defined

$$\mu_S = \left( \frac{\partial T}{\partial p} \right)_S = \frac{T}{c_p} \left( \frac{\partial v}{\partial T} \right)_p. \quad (4.55)$$

Here the derivative in the second form corresponds to the volumetric coefficient of thermal expansion  $\beta$ , which is always positive for gases, which in turn means, that an isentropic expansion will always result in an temperature decrease, whereas the isenthalpic expansion only led to a decrease in certain cases. Furthermore an isentropic expansion over the same pressure range will always result in lower temperatures than an isenthalpic expansion. Additionally work can be recovered. The reason that isentropic valves are most commonly used in liquefaction systems, is that those work producing machines cannot handle significant phase changes, which is after all the desired result of liquefaction.

Traditionally only the isenthalpic expansion had been used within the cryogenic air separation process, since – as mentioned before – the air needs to be liquefied in order to be fed into be distilled. However in modern process configurations the isentropic expansion is also considered, and partial streams are fed into the low pressure column in gaseous form.

## 4.2 Dynamic unit models

### 4.2.1 Distillation column model

The previously described column model is based on a steady state assumption. This means that all variables do not change with time. While a model like that offers valuable insight into the operation

explain  
model  
assump-  
tions.

of a process many aspects remain unclear. In order to gain further insight into the process the dynamics have to be considered.

Due to that in this section a dynamic model of the ASU process will be developed.

First the balance equations have to be rewritten in dynamic form. To do so reservoir terms or holdups are introduced. Namely the component holdups  $n_{ij}$  and internal energy  $U_j$  for each stage. with that the component balance equations as presented in the previous section can now be rewritten as

$$\begin{aligned} \left(1 - \sum_{k=1}^{j-1} \zeta_k^R\right) \frac{dn_{ij}}{dt} = & (1 + s_j^V) \cdot V_j \cdot y_{ij} + (1 + s_j^L) \cdot L_j \cdot x_{ij} - V_{j+1} \cdot y_{ij+1} \\ & - L_{j-1} \cdot x_{i,j-1} - \sum_{l=1}^{n_F} \zeta_{lj} \cdot F_j \cdot z_{lj} - \zeta_j^R \cdot V_N \cdot y_{iN}, \\ i = 1 \dots n_C - 1, \quad j = 1 \dots N, \quad k = 1 \dots n_F, \quad l = 1 \dots n_F. \end{aligned} \quad (4.56)$$

While the internal energy balances become

$$\begin{aligned} \left(1 - \sum_{k=1}^{j-1} \zeta_k^R\right) \frac{dU_j}{dt} = & (1 + s_j^V) \cdot V_j \cdot h_j^V + (1 + s_j^L) \cdot L_j \cdot h_j^L - V_{j+1} \cdot h_{j+1}^V \\ & - L_{j-1} \cdot h_{j-1}^L - \sum_{k=1}^{n_F} \zeta_{kj} \cdot F_k \cdot h_j^F - \zeta_j^R \cdot V_N \cdot h_N^V, \\ i = 1 \dots n_C, \quad j = 1 \dots n, \quad k = 1 \dots n_F, \quad l = 1 \dots n_F. \end{aligned} \quad (4.57)$$

In addition to the balance equations further constituent equations need to be introduced. From the steady state model we know the equilibrium equations

$$y_{ij} = K_{ij} \cdot x_{ij}, \quad i = 1 \dots n_C \quad j = 1 \dots n_S, \quad (4.58)$$

and the summation equations

$$1 = \sum_i^{n_C} y_{ij} \quad j = 1 \dots n_S, \quad (4.59)$$

$$1 = \sum_i^{n_C} x_{ij} \quad j = 1 \dots n_S. \quad (4.60)$$

Furthermore the accumulation of moles in each stage in vapour  $n_j^V$  and liquid  $n_j^L$  need to be considered with

$$n_{ij} = x_{ij} n_j^L + y_{ij} n_j^V \quad i = 1 \dots n_C \quad j = 1 \dots n_S, \quad (4.61)$$

$$(4.62)$$

These holdups are linked by the volume of a given stage  $V_{stage}$ . Thus the volume constraint can be written as

$$V_{stage} = \frac{n_j^V}{\rho_j^V} + \frac{n_j^L}{\rho_j^L} \quad j = 1 \dots n_S. \quad (4.63)$$

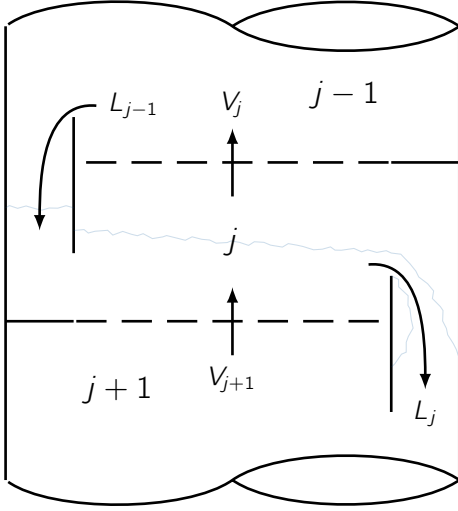


Figure 4.9: Column tray

The internal energy in a stage corresponds to its enthalpy, reduced by pressure term

$$U_j = n_j^L \cdot h_j^L + n_j^V \cdot h_j^V - p_j \cdot V_{stage} \quad (4.64)$$

As we are no longer dealing in steady state hydraulic equations need to be introduced, which determine the liquid and vapour flow rates leaving a separation stage. As the mechanisms driving these flows might be very different depending on the type of internals used, it is not surprising that the corresponding equations are also very different. In the given model both trayed columns and columns with structured packing are employed.

### Trayed hydraulics

Trayed column hydraulics can be approximated by the following system of equations. All equations presented here were taken from [16].

The liquid flow rates are calculated from the well established Francis formula, derived from the law of Bernoulli and taking effects like bubbling into account

$$L_j = \frac{2}{3} \sqrt{2g} \rho_j^L \ell_{weir} \Phi h_{ow}^{\frac{3}{2}} \quad j = 1 \dots n_S. \quad (4.65)$$

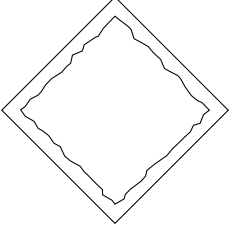
Where  $h_{ow}$  denotes the height of the liquid over the weir, which can be calculated from the froth height  $h_f$  and the weir height  $h_w$

$$h_{ow} = h_f - h_w. \quad (4.66)$$

While the weir height is a tray design parameter the froth height is computed from the clear liquid height and the relative froth density

$$h_f = \frac{n^L MW^L}{A_{active} \rho^L \Phi}. \quad (4.67)$$

add  
graphic  
for tray  
meas-  
ure-  
ments.



Lastly in terms of liquid flow rates, the relative froth density is dependent on the degree of aeration within the liquid, expressed by the aeration factor  $\beta$  from an empirical equation

$$\beta_j = 1 - 0.3593 \left( \frac{V_{j-1} MW_{j-1}^V}{A_{active} \sqrt{\rho_{j-1}}} \right)^{0.177709} \quad j = 1 \dots n_S, \quad (4.68)$$

$$\Phi_j = 2\beta_j - 1. \quad (4.69)$$

The pressure difference between stages is the driving force for the vapour streams. The pressure drop is modeled as having two contributions, the dry and wet pressure drop. While dry pressure drop stems from the vapour flowing through the holes with in tray, the wet pressure drop is caused by the liquid holdup on the stage.

$$p_j - p_{j+1} = h_j^{liq} \rho_j^L g + 0.5 \xi \rho_{j+1}^V \left( \frac{q_{j+1}^V}{A_h} \right)^2 \quad (4.70)$$

### Structured packing hydraulics

write somewhere that stage indices will be omitted for convenience.

Structured packings and their hydraulic behaviour are currently still under investigation. The number of available correlations for calculation of internal flow-rates is much more limited than for trays or even dumped packings. Among the most established models is the one developed by Bravo et al. [22] at the University of Texas. This model has been extended to be valid in the loading region and account for different types of packing material [13]. As main linking factor between vapour and liquid flow-rates as well as the pressure drop, the liquid holdup has been identified by the authors. It is expressed in dimensionless form  $h_t$  in terms of the corrugation side  $S$ , and the film thickness  $\delta$

$$h_L = \frac{4}{S} \delta. \quad (4.71)$$

One very important factor while estimating the hydraulic behaviour is the dry pressure drop per meter packing  $\delta p_{dry}$ . Within in the presented model it is estimated by

$$\delta p_{dry} = \left( \frac{\rho^G}{\rho_{air,1bar}} \right)^{0.4} \left( \frac{C_1 \rho^G v_G^2}{S \epsilon^2 (\sin \Theta)^2} + \frac{C_2 \mu_G v_G}{S^2 \epsilon \sin \Theta} \right) \quad (4.72)$$

Another prerequisite for calculating the holdup is the knowledge of the amount of wetted area of the available surface area within the packing. It seems reasonable to assume that this will be dependent

on the characteristic of the liquid flow through the packing. To characterize the current, well known dimensionless numbers are used. Namely *Weber* ( $We$ ), *Froude* ( $Fr$ ) and *Reynolds* ( $Re$ ) numbers

$$We = \frac{v_L^2 \rho_L S}{\sigma}, \quad (4.73)$$

$$Fr = \frac{v_L^2}{Sg}, \quad (4.74)$$

$$Re = \frac{v_L S \rho_L}{\mu_L} \quad (4.75)$$

With that an approximation for the holdup correction factor  $F_t$  due to partial wetting can be expressed as

$$F_t = \frac{A_1 (We Fr)^{0.15} S^{A_2}}{Re^{0.2} \epsilon^{0.6} (1 - 0.93 \cos \gamma) (\sin \Theta)^{0.3}} \quad (4.76)$$

$$h_L = \left( \frac{4F_t}{S} \right)^{\frac{2}{3}} \left\{ \frac{3\mu_L v_L}{\rho_L \epsilon \sin \Theta g \left[ \left( \frac{\rho_L - \rho_G}{\rho_L} \right) \left( 1 - \frac{\delta p}{\delta p_{flood}} \right) \right]} \right\}^{\frac{1}{3}} \quad (4.77)$$

## 4.2.2 Integrated condenser / reboiler unit

As it has been stated on several occasions the condenser reboiler unit is essential in the cryogenic air separation process. When it comes to dynamics the pressure profile deserves much attention, as it is crucial for feasible operations of the entire process. The pressure difference between the low and high pressure column enables the heat exchange in this unit.

## 4.3 Sizing & costing models

As discussed earlier economic consideration play a major role in process design. In order to account for the process economics the cost of the process to be implemented needs to be estimated at the design level. However as limited information is available estimation methods have to be employed. In sec. 3 the general approach for cost estimation of process equipment was introduced, where a specific value such as heat-exchange area or vessel size is used to approximate equipment cost. However for more specific units extended models are available, where statistical data is employed to yield a more realistic fit to cost data. The cost functions and correction factors presented in this chapter are, if not stated otherwise, taken from [23]. Also unless otherwise stated the unit cost is given for the year 2006 ( $CE = 500$ ).

mention  
delft,  
sti,  
hydro-  
dynamic  
con-  
tinuum

include  
Integ-  
rated  
con-  
denser  
/  
re-  
boiler  
unit

### 4.3.1 Distillation column

The cost of a given distillation column  $C_{\text{column}}$  is comprised of three main parts, the cost for the vessel or tower itself  $C_{\text{tower}}$ , the cost for platforms, ladders, manholes, and nozzles  $C_{\text{platform}}$  and the cost for the internals  $C_{\text{internals}}$

$$C_{\text{column}} = C_{\text{tower}} + C_{\text{platform}} + C_{\text{internals}}. \quad (4.78)$$

The determining factors for the cost of a tower are the construction material and the weight of the vessel. The material is considered by multiplying a base cost by a material factor  $f_M$ . Thus the cost for the tower can be approximated by

$$C_{\text{tower}} = f_M \cdot \exp \left[ 7.2756 + 0.18255 \cdot \ln(W_{\text{tower}}) + 0.02297 \cdot (\ln(W_{\text{tower}}))^2 \right], \quad 9000 \leq W_{\text{tower}} \leq 2.5 \cdot 10^6. \quad (4.79)$$

In this correlation the weight  $W$  is measured in pounds ( $[lbs]$ )

For the support structures the following equation has been presented

$$C_{\text{platform}} = 300.9 \cdot (d_{\text{column}})^{0.63316} \cdot (l_{\text{column}})^{0.80161}, \quad (4.80)$$

where both the diameter  $d_{\text{column}}$  and length  $l_{\text{column}}$  are measured in feet ( $[ft]$ ).

The weight of the column is attained by calculation its volume and multiplying it by the mass density of the construction material  $\tilde{\rho}$

$$W_{\text{column}} = \pi(d_{\text{column}} + t_s)(l_{\text{column}} + 0.8 \cdot d_{\text{column}})t_s \cdot \tilde{\rho}. \quad (4.81)$$

It needs to be noted, that in this formula, all measurements have to be adjusted to the measurement of the density. Newly appearing is the shell thickness  $t_s$  of the tower. In order to compute this, several aspects can be considered.

The ASME pressure vessel code formula is used to compute the minimum thickness due to the design pressure  $p_D$  of a tower

$$t_p = \frac{p_D d_{\text{column}}}{2 S E - 1.2 p_D}, \quad (4.82)$$

where  $S$  denotes the maximum allowable stress and  $E$  the fractional weld efficiency.

The design pressure is computed from the operating pressure  $p_O$

$$p_D = \max \left\{ 10, \exp \left[ 0.60600 + 0.91615 \cdot \ln(p_O) + 0.0015655 \cdot (\ln(p_O))^2 \right] \right\}, \quad (4.83)$$

It should be pointed out the the pressures in the previous equation are measured in pound per square inch gauge ( $[psig]$ ).



In addition to the thickness due to pressure, it should be considered – especially for tall vessels – that the vessel might have to withstand external forces such as strong winds or earthquakes. To account for external effects a security addition  $t_w$  to the pressure thickness can be computed

$$t_w = \frac{0.22(d_{\text{column}} + 18)l_{\text{column}}^2}{Sd_{\text{column}}}. \quad (4.84)$$

Therefor the total shell thickness amounts to

$$t_s = t_p + t_w. \quad (4.85)$$

In the previous equations the column diameter and length have frequently been used, however no mention has been made as to how to attain these values. While for a given design these values will be fixed, in the context of an optimization they need to be considered as decision variables. These decisions are closely linked to the choice of column internals. In case of the column height the procedure is very similar for columns with trays and structured packings. In case of the diameter however a clear distinction has to be made. This is due to the fact, that a decision regarding the diameter will have to ensure feasible column operations, which means it will have to be large enough to avoid flooding within the column. Consequently the procedures for determining height and diameter will be dealt with separately for each type of internals.

## Trays

For a trayed column the height can be determined from the number of stages  $n_S$  used multiplied by the plate spacing  $h_{\text{plate}}$ . In addition however it needs to be ensured, that control of the columns is still possible. At the sump of the tower liquid will accumulate during operations. While in an ideal case the liquid level would be constant, that cannot be assumed. Regularly there are three different liquid levels defined in a column. The high level (HLL), normal level (NLL) and the low level (LLL). These levels are defined such that it sufficient time for the liquid to reach these levels  $(t_{\min}^{\text{HLL}}, t_{\min}^{\text{NLL}}, t_{\min}^{\text{LLL}})$ , if no liquid id withdrawn anymore, or no liquid comes down from the column. Furthermore the times for reaching the reboiler inlet and the lowest plat will ne necessary. What duration to reach those levels will be sufficient needs to be decided by a control engineer.

With these times and heights the height of the tower can be expressed as

$$l_{\text{column}} = n_S \cdot h_{\text{plate}} + \left( \sum_i t_{\min}^i H^i \right) \cdot \frac{L_{n_S}}{A_{\text{column}} \varrho^L}. \quad (4.86)$$

This leaves the diameter to be determined. The most important factor to that regard is the vapour velocity within the tower. It is to be chosen such that no flooding or entrainment will occur. The following equation to compute these operation boundaries are taken from [17].

First the fractional entrainment factor  $ent_j$  for 80% flooding at each stage  $j$  needs to be calculated

$$ent_j = 2.24 \cdot 10^{-3} \cdot 2.377 \exp \left[ -9.394 \cdot FLV_j^{0.314} \right], \quad j = 1 \dots n_S. \quad (4.87)$$

Therein the Sherwood flow parameter  $FLV_j$  is used

$$FLV_j = \frac{\tilde{L}_j}{\tilde{V}_j} \cdot \sqrt{\frac{\tilde{\rho}_j^V}{\tilde{\rho}_j^L}}, \quad j = 1 \dots n_S. \quad (4.88)$$

$$v_j^{flood} = 60 \cdot \left( \frac{\sigma_j^L}{20} \right)^{0.2} \cdot K1_j \cdot \sqrt{\frac{\tilde{\rho}_j^L - \tilde{\rho}_j^V}{\tilde{\rho}_j^V}}, \quad j = 1 \dots n_S. \quad (4.89)$$

$$K1_j = 1.05 \cdot 10^{-2} + 0.1496 \cdot h_{plate}^{0.755} \cdot \exp[-1.463 \cdot FLV_j^{0.842}], \quad j = 1 \dots n_S. \quad (4.90)$$

With those values the minimum required column area for each stage  $A_j^{min}$  can be calculated

$$A_j^{min} = \frac{V_j}{\Psi_{flood} \tilde{\rho}_j^V v_j^{flood}}, \quad j = 1 \dots n_S, \quad (4.91)$$

where  $\Psi_{flood}$  is a design parameter which determines the degree of flooding allowed and will usually have a value around 0.8.

## Structured packings

The calculation of the column height is equivalent to the trayed case, with the one difference, that rather than using the plate spacing as the height for each stage a value called height equivalent to theoretical plate (*HETP*) is used. In terms of the column diameter the flooding velocity is determined by the flooding pressure drop as calculated in sec. 4.2.1.

### 4.3.2 Centrifugal pump

Pumps are among the most common units of process equipment. While there are several different kinds of pumps that can be used, the centrifugal pump is one of the most popular choices and denotes a very likely choice for the process conditions considered in this application. Hence other pump types will not be considered at this point.

check  
time  
con-  
stant  
(60) for  
flood-  
ing  
velocity

check  
results  
for min-  
imum  
column  
dia-  
meter  
when  
using  
flood-  
ing  
pres-  
sure  
drop,  
or fit-  
ted  
flood-  
ing

#### 4 Mathematical process model

| number of stages | shaft rpm | case-split orientation | flow rate range ([gpm]) | pump head range ([ft]) | maximum power ([Hp]) | type factor $f_T$ |
|------------------|-----------|------------------------|-------------------------|------------------------|----------------------|-------------------|
| 1                | 3600      | VSC                    | 50 - 900                | 50 - 400               | 75                   | 1.00              |
| 1                | 1800      | VSC                    | 50 - 3500               | 50 - 200               | 200                  | 1.50              |
| 1                | 3600      | HSC                    | 100 - 1500              | 100 - 450              | 150                  | 1.70              |
| 1                | 1800      | HSC                    | 250 - 5000              | 50 - 500               | 250                  | 2.00              |
| 2                | 3600      | HSC                    | 50 - 1100               | 300 - 1100             | 250                  | 2.70              |
| 2+               | 3600      | HSC                    | 100 - 1500              | 650 - 3200             | 1450                 | 8.90              |

Table 4.3: Pump type factors [23].

| material of construction | material factor |
|--------------------------|-----------------|
| cast iron                | 1.00            |
| ductile iron             | 1.15            |
| cast steel               | 1.35            |
| bronze                   | 1.90            |
| stainless teel           | 2.00            |
| Hastelloy C              | 2.95            |
| monel                    | 3.30            |
| nickel                   | 3.50            |
| titanium                 | 9.70            |

Table 4.4: Pump material factors [23].

**Pump** In terms of operations pumps are best described by the volumetric flow transported  $Q$  as well as the pump head  $H$ , the hight that needs to be overcome. Data taken from the company Mosanto was used to correlate the pump cost to a specific value

$$S = Q\sqrt{H}. \quad (4.92)$$

As a reference unit the base price  $C_B$  is estimated for a cast iron single-stage vertically split case at 3600 rpm

$$C_B = \exp \{9.7171 - 0.6019 \cdot \ln[S] + 0.0519(\ln[S])^2\}, \quad 400 \leq S \leq 100000. \quad (4.93)$$

The most influential addition factors for the pump price are the material, which is accounted for in the material factor  $f_m$ , as well as the rotation, case split orientation (horizontal and vertical), the number of stages, covered flow rate range, pump head range and maximum motor power, which are all agglomerated in the type factor  $f_T$ . Values for these factors are given in tab. 4.3 and tab. 4.4.

**Electric motor** Separately from the pump itself the motor to drive the compression is considered. While the volumetric flow and the pump head certainly are valid choices to correlate motors for pumps especially, the power consumption is a more general specific value

$$P_C = \frac{P_T}{\eta_P \eta_M} = \frac{P_B}{\eta_M} \quad (4.94)$$

It can be calculated from the theoretic power of the pump  $P_T$  and the efficiencies  $\eta_P$   $\eta_M$ . While an estimate for the expected power consumption might be already available at rather early design

| type motor enclosure                      | 3600 rpm | 1800 rpm |
|---|----------|----------|
| open, drip-proof enclosure, 1 to 700 Hp   | 1.0      | 0.9      |
| totally enclosed, fan-cooled, 1 to 250 Hp | 1.4      | 1.3      |
| explosion-proof enclosure, 1 to 250 Hp    | 1.8      | 1.7      |

Table 4.5: Type factors for different motor types.

stages, the efficiencies will have to be correlated as well if resorting to average values is considered too coarse. Those correlations rely on the volumetric flow in gallons per minute ([gpm]) and the brake horse power  $P_B = \frac{P_T}{\eta_P}$ .

$$\eta_P = -0.316 + 0.24015 \cdot \ln[Q] - 0.01199 \cdot (\ln[Q])^2 \quad 50 \leq Q \leq 5000 \quad (4.95)$$

$$\eta_M = 0.80 + 0.0319 \cdot \ln[P_B] - 0.00182 \cdot (\ln[P_B])^2 \quad 1 \leq P_B \leq 1500 \quad (4.96)$$

After having calculated the power which the motor needs to supply its base cost of an open, drip-proof enclosed motor at 3600 rpm can be approximated by

$$C_B = \exp \left\{ 5.8259 + 0.13141 \cdot \ln[P_C] + 0.053255 \cdot (\ln[P_C])^2 + 0.028628 \cdot (\ln[P_C])^3 - 0.0035549 \cdot (\ln[P_C])^4 \right\} \quad 1 \leq P_C \leq 700 \quad (4.97)$$

To adjust the cost for different types of electric motors the type factors from tab. 4.5

## Compressor

The cost of compressors is correlated with their respective power consumption measured in horsepower. Although not the most efficient type of compressor, centrifugal compressors are very popular in the process industry, as they are easily controlled and deliver a very steady flow. However as different types might be employed as well base cost correlations for centrifugal, reciprocation and screw compressors are given.

### Centrifugal compressor

$$C_B = \exp \left\{ 7.5800 + 0.80 \cdot (\ln[P_C]) \right\} \quad 200 \leq P_C \leq 30000 \quad (4.98)$$

### Reciprocating compressor

$$C_B = \exp \left\{ 7.9661 + 0.80 \cdot (\ln[P_C]) \right\} \quad 200 \leq P_C \leq 20000 \quad (4.99)$$

### Screw compressor

$$C_B = \exp \{8.1238 + 0.7243 \cdot (\ln[P_C])\} \quad 200 \leq P_C \leq 750 \quad (4.100)$$

Again as with most other equipment types correction factors are used to adjust for different realization of this piece of equipment. Here type of motor as well as the construction material have the biggest effects on the unit price and are explicitly considered.

$$C_p = f_D f_M C_B \quad (4.101)$$

The alternatives to the electric motor ( $f_D = 1.0$ ) are a steam turbine ( $f_D = 1.15$ ) or a gas turbine ( $f_D = 1.25$ ). It should however be noted that aside from being the cheapest choice, the electric motor is also the most efficient. Thus the turbines are mostly considered, when process steam or combustion gas is easily available, such that the drawbacks might be eliminated by not having to supply the electric energy for the electric motor. In terms of construction material all base costs are for cast iron or carbon steel. Some appliances may require more resistant and also more expensive materials such as stainless steel ( $f_M = 2.5$ ) or an nickel alloy ( $f_M = 5.0$ ).

### Reboiler / condenser

Reboiler and condenser can be characterized as heat exchangers, and be handled in the same way, as the main difference is whether heat is transferred to or from the process stream. In that sense they must be distinguished when considering the operating cost, as the cost for hot or cold auxiliary streams might differ significantly. As customary for heat exchangers the specific quantity for cost correlations is the necessary heat exchange area  $A$  measured in  $ft^2$ .

Again the construction material as well as the operating conditions have an effect on the final cost

$$C_p = f_P f_M C_B. \quad (4.102)$$

The correction for pressures  $f_P$  takes into account the operating pressure  $P_o$  and is computed by

$$f_P = 0.8510 + 0.1292P_o + 0.0198 * P_o^2. \quad (4.103)$$

The material correction factor  $f_M$

$$f_M = \quad (4.104)$$

### Shell and tube heat exchanger

$$C_B = \exp \{11.667 - 0.8709 \cdot (\ln[A]) + 0.09005 \cdot (\ln[A])^2\} \quad (4.105)$$

### Double pipe

$$C_B = \exp \{7.146 + 0.1600 \cdot (\ln[A])\} \quad (4.106)$$

## 4.4 Thermodynamic models

Aside from the unit operation models, the behaviour of materials in a process needs to be adequately accounted for. This is done by means of so called equations of state (EOS) and excess Gibbs energy models. In terms of thermodynamics there are only a limited amount of variables. Namely the pressure, density and temperature as well as composition. While equations of state can model a given system in the vapour as well as liquid phase, excess Gibbs energy models only account for the behaviour of a liquid and need to be used in conjunction with other models for the vapour phase. However they have shown considerable better performance for highly non-ideal systems [2]. As mentioned earlier (sec. ??) it is essential to accurately capture the non-idealities of air in order to capture the liquefaction process. In the case of cryogenic air separation, the Peng-Robinson as well as the Benders equation of state have shown satisfactory performance. The Peng-Robinson equation was chosen to be used in the presented model

$$p = \frac{RT}{V - b} - \frac{a_c [1 + m(1 - \sqrt{T_r})]^2}{V^2 + 2bV - b^2} \quad (4.107)$$

$$m = 0.37464 + 1.54226\omega - 0.26992\omega^2 \quad (4.108)$$

$$a_c = 0.45724 \frac{R^2 T_c^2}{p_c} \quad (4.109)$$

$$b = 0.077796 \frac{RT_c}{p_c} \quad (4.110)$$

$$\omega = -1 - \log_{10}(p_r^{sat})_{T_r=0.7} \quad (4.111)$$

However the Peng-Robinson EOS relies on the so called one-fluid theory which models each fluid as pure. To model mixtures the pure component parameters have to be "mixed"

$$a = \sum_{i=1}^C \sum_{j=1}^C y_i y_j a_{ij}, \quad (4.112)$$

$$a_{ij} = \sqrt{a_i a_j} (1 - k_{ij}), \quad (4.113)$$

$$b = \sum_{i=1}^C y_i b_i. \quad (4.114)$$

From that EOS numerous relevant properties such as excess enthalpy, fugacity coefficients or densities can be calculated. For a list of some relevant equations refer to sec. A.1.

## 4.5 Implementation

As mentioned the presented models have been implemented in the process simulator gPROMS<sup>®</sup>. Although application to the cryogenic air separation process served as case where the model would be applied, the aim was to develop – especially in the case of the column models – a flexible model

which properties should be included? Or move everything to Appendix?

which could be used for a multitude of problems while trying to achieve a reasonable amount of complexity, such that a user mainly used to a pure flowsheeting environment should be able to apply the models with relative ease.

In the following sections first some general aspects of modeling in gPROMS<sup>®</sup> will be pointed out and the structure of the implemented model discussed in more detail. Subsequently several strategies for initializing the column model based on the previously model structure will be presented.

### 4.5.1 Model structure

When discussing the structure of gPROMS<sup>®</sup> models first some aspects of the modeling language have to be discussed. In this context CASE selectors, IF statements and the implementation INITIALIZATION\_PROCEDURE's in gPROMS<sup>®</sup> are most important. Within this section we will first briefly discuss those features and how they are used in gPROMS<sup>®</sup>. Afterwards it will be shown, how these structures are used, to create a model which can quickly be tailored the specific needs of a given user, and how distillation columns can be initialized within that framework.

IF statements and case selectors have many similarities as they can distinguish between different cases within a given model. For many applications they might even be used equivalently. As in almost all contexts the IF statements evaluates a condition and depending on whether it is fulfilled or not and evaluates different formulae accordingly. A CASE statement distinguishes different branches between the model can switch during simulation or initialization. One major difference is, that the number of equations in each CASE branch must match while for IF statements that condition is not enforced. However care must be taken when using these structures – especially during simulation – as they will in many cases introduce discontinuities. Furthermore when using IF statements one must distinguish, whether the evaluated statement is a parameter, or a variable in the model. Given it is a parameter, the statement will remain true (or false) for each instance of simulation. This introduces some flexibility in terms of diverging in the number of equations within model variants.

INITIALIZATION\_PROCEDURE's are used – as the name suggests – to initialize models. The basic idea is to automatically solve a sequence of increasingly complex models, using the solution of a previous model as starting point for converging the current one. Furthermore the switch between models can be done within a either a so called JUMP\_TO or MOVE\_TO statement. Within the former there is a hard cut between the model variants, while in the latter a homotopic approach is employed to get from one model branch to another. While this should be the more robust solution, if the path of the homotopy remains in a feasible region, it necessitates greater care in terms of model robustness and scaling, as the internal integrator is used to move along the homotopic path.

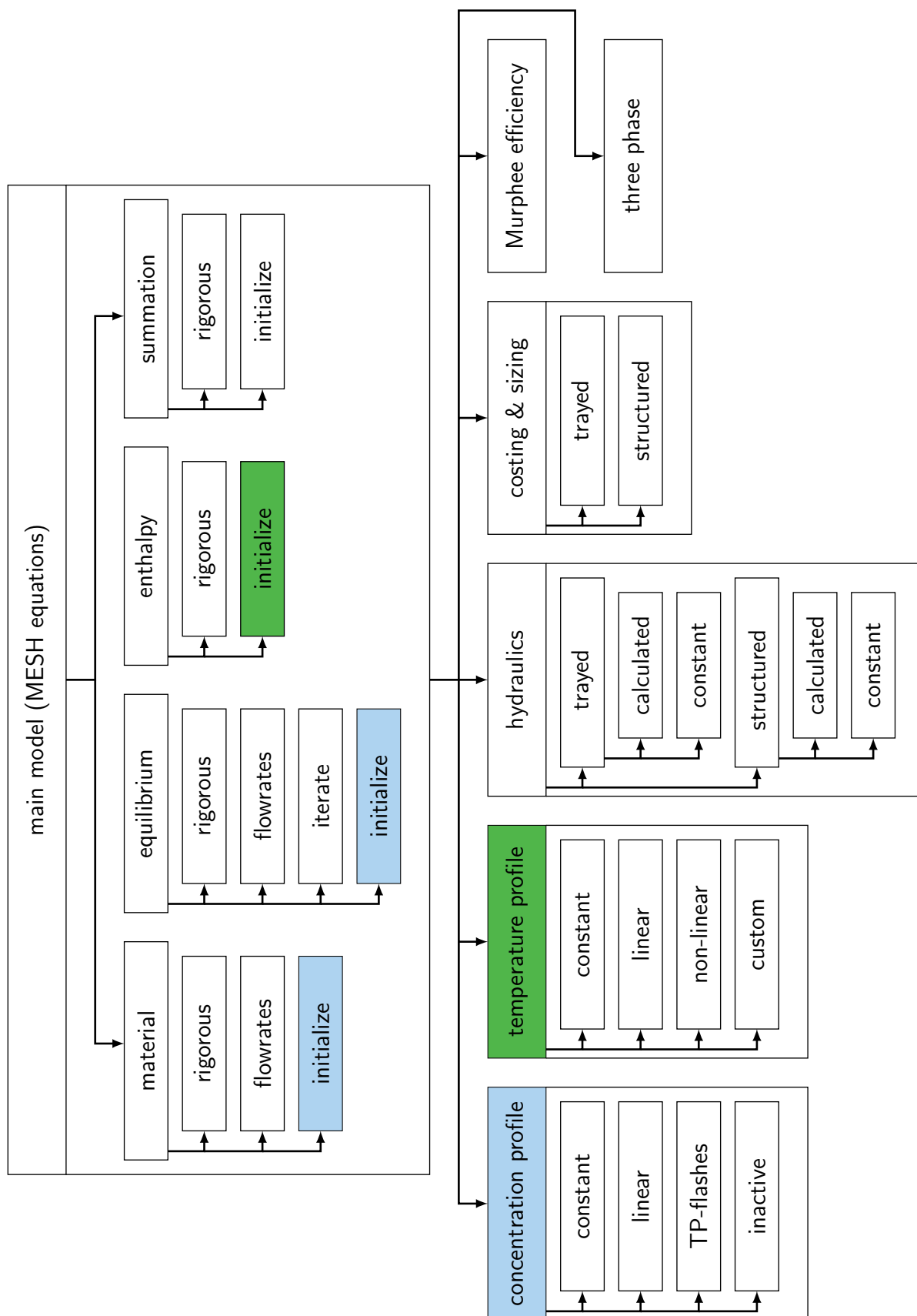


Figure 4.10: Distillation column model structure including sub-models and CASE branches.



include  
initial  
speci-  
fica-  
tions in  
model  
struc-  
ture

The structure of the developed model is depicted in fig. 4.10. The main block denote separate model units that can, with the exception of the main model be activated or deactivated. The connections inside the main blocks denote selectors along with their possible branches.

The selective deactivation of sub-models is done by creating sub flowsheets and then assigning array of a respective model rather than a specific entity. By assigning an array size of zero, the model is effectively deactivated. This is done to reduce the number of variables and computational effort, if certain model capabilities are superfluous. for the rest of this section various model branches will be briefly elaborated upon. Within the main model, all branches labeled "rigorous" correspond to the equations as presented in sec. 4.1.1 and sec. 4.2. For the "flowrates" branches the mass balance has been written in terms of component flowrates rather than total flowrates and mole fractions. The "initilaize" branches of the material, equilibrium and energy selectors rely on the concentration profile and temperature profile sub-models to generate values, which are assigned straight forward to the respective variables. The reason those guesses were not directly implemented in the main model was to retain a level of flexibility of implementing alternative approaches without altering the general model structure. The meaning of the "iterate" branch within the equilibrium selector will be discussed in further detail in the next section.

The profile sub-models give several choices for initial profiles. In the case of the concentration profiles, the edge points will always be determined by a TP or vapour fraction flash of the mixed feed. While for temperature profile model the edge points can be either bubble and dew point temperature of the mixed-feed, or the feed temperatures of the highest (in terms of feed location) and lowest feed.

Having variable pressure along the column, sometimes greatly complicates initial convergence. Therefore can all hydraulics models be turned inactive, in which case they will return a constant previously assigned pressure drop for each stage.

The sub-model "three-phase" somewhat emulates calculations for the case when to liquid phases are present, as it needs to be ensured, that no wrongful information about the phase equilibrium is attained b y the model, which can for instance cause severe errors in the mass balance, while the overall model might still converge. It is simply assumed, that the liquid phases, while separate, are distributed in such a way, that the liquid phase might still be treated as a single phase. Hence in that case, the concentrations and enthalpies of both phases are mixed, while information about both phases is stored in appropriate variables.

## 4.5.2 Initialization procedures

This section deals with different initialization strategies for the distillation columns. Before going deeper into that topic, it needs to be pointed out, that physical property estimation in gPROMS<sup>®</sup> is done by means of so called foreign objects. Those are external objects, to which function calls along with the corresponding parameters can be passed and a return value or vector is returned. These calls range from simple properties like molecular weight of components to flash calculations in many variations.

include  
gPROM  
code  
for IP's

mention  
TP  
flashes  
branch  
of  
concen-  
tration  
sub-

As an initial remark it should be noted, that for all initialization procedures, if the hydraulic sub-model is activated, first an initial profile is assumed, and after the model has converged, the selector within the hydraulics sub-model is switched to the calculated pressure drops. No problems with the hydraulics models were encountered, if the specified column geometry allowed for feasible column operations.

### Initial specifications

One issue that comes up when giving specifications for a column is, that not all specifications are compatible with the the used initialization procedure. Specifically this is the case for specified duties purities or temperatures as they cannot be considered in the initialize branches.

For those cases it is necessary to supply alternative specifications, namely a reflux or boil-up ratio or any flowrate, which can be fulfilled during initial calculations. Additionally, if "extreme" specifications are given such as very high purities, or extremely low flowrates, convergence might with a given procedure might fail. One strategy, that has proven fruitful in those cases, was to supply a more moderate specification, initialize and converge the model up to the rigorous branches and then switch to the more complex specification. Especially when the switch is made in the rigorous branch, chances are high, that the solution, if a MOVE\_TO switch is employed, will only pass through feasible regions and a final solution can be attained.

These initial specification can be used in conjunction with all initialization procedures discussed in the following sections.

### Flash initialization

The flash initialization, is the simplest, but nevertheless a very effective and efficient way of initializing the model. As initial guess constant profiles are assigned for vapour and liquid concentrations taken from the aforementioned feed flash. For the temperatures a linear profile between dew and bubble point temperature of the feed flash is used. The vapour and liquid flowrates are computed from the constant molar overflow assumption while considering sub-cooled or super-heated feed streams. In terms of the model this strategy translates into starting all selectors in the initialize branches and then simultaneously switching all selectors to the rigorous branches.

### Linearized material balance

As discussed in the example given in sec. 4.1.1 this initialization procedure relies on on first initializing the model as for the flash initialization. Afterwards, in an intermediate step, the enthalpy and summation branch are kept in the initialize branch, which means, the initial temperature profile is kept fixed, and the constant molar overflow assumption retained. The material and equilibrium selectors are then switched to the flowrates branches, where a linearized material balance is solved with constant equilibrium ratios and molar flowrates. The constant equilibrium ratios are enforces, by passing the values from the concentration profile sub-model to the physical property calls, rather than the actual computed values for molar concentrations.

The main reason for formulating this mass balance in terms of component flowrates is, that due to the assumptions a solution will yield discrepant results. Especially if the equilibrium ratios in the converged solution span a large range of values. Due to these discrepancies some molar fractions might even become negative. As the corresponding variable type is bounded to zero or a small negative number, this might cause the solver to fail during convergence of this step.

Furthermore the molar fractions would also have to be re-normalized, as the summation to one is not enforced in this case.

Afterwards all selectors are again switched to the rigorous branch.

#### INITIALISATION\_PROCEDURE

```
START
  material      := initialize ;
  equilibrium   := initialize ;
  energy        := initialize ;
  summation     := initialize ;
  side_scale    := 0 ;
  hydraulics    := constant ;
END
NEXT
  material      := flowrates ;
  equilibrium   := flowrates ;
END
NEXT
  REVERT material ;
  REVERT equilibrium ;
  REVERT energy ;
  REVERT summation ;
END
NEXT
  MOVE_TO
    side_scale := 1 ;
  END
END
NEXT
  REVERT hydraulics ;
END
```

### Iterative approach

Previously it has been said, that the inside-out algorithm has proven very robust when it comes to solving complex distillation problems. However it is based on an modular iterative approach which is incompatible with equation based process simulators.

One of the main aspects is to construct simplified models for enthalpies and the equilibrium, which only give accurate results for the point they have been constructed at, but are much better behaved,

than rigorous enthalpy and equilibrium correlations. In each step of the iteration a new model for the physical properties is constructed, at the point, where the previous model evaluation with the previous physical properties model converged to. The iterative process terminates, when no further (or very little) changes occur in the newly constructed parameters for the new physical property models.

In order to mimic such an approach in gPROMS<sup>®</sup>, the branch "iterate" within the equilibrium selector has been created. There the physical properties are called with an new set of concentration variables, which are assigned arbitrary values in all other branches. To do the iterations another structure of gPROMS<sup>®</sup> is used. So called TASKS. With that it becomes possible, to converge a the model, with a given concentration stored in these variables, and after convergence, replace those values with the current values of liquid and vapour mole fractions.

The drawback however, is that the number of iterations to be carried out needs to be specified in advance. This strategy, while rather time consuming due to large overhead in computational time during execution of the TASK, has generated very promising results and with it it was possible to converge columns with very complex multi-component systems.

```

SEQUENCE
  i := 1 ;
  WHILE i < number_of_iterations DO
    SEQUENCE
      PARALLEL
        REASSIGN
          column_section.x_iterate(,) := OLD(column_section.x(,));
          column_section.y_iterate(,) := OLD(column_section.y(,));
        END
      SWITCH
        column_section.phase_equilibrium
          := column_section.iterate_to_rigorous;
      END
    END
    i := i + 1 ;
  END
END
SWITCH
  column_section.phase_equilibrium := column_section.rigorous;
END
END

```

### Side draws

During construction of process flowsheets and application of the developed models it turned out, that columns with side draws add extra complexity in terms of initialization. To accommodate that fact side draw versions of the previously described initialization procedures have been developed. The only

difference is, that the side draws are initially set to zero once convergence has been achieved, they are again set to their specified values. Either by an instant change or again in a continuous fashion.

# Todo list

|   |    |
|---|----|
| ■ briefly discuss general process steps. mention pre-purification. . . . .  | 17 |
| ■ find appropriate place for integrated reboiler condenser unit. . . . .  | 17 |
| ■ add flowsheet initialization from MathModel file . . . . .  | 17 |
| ■ add side draws to column super structure . . . . .  | 18 |
| ■ section superfluous? init procedure describen in impl sec... . . . .  | 23 |
| ■ elaborate on adiabatic column . . . . .   | 25 |
| ■ mention problems and bounded homotopy? . . . . .  | 28 |
| ■ adjust heat exchange section to current approach. . . . .   | 30 |
| ■ add citation Lindhoff... . . . .  | 30 |
| ■ elaborate on pinch concept? . . . . .   | 30 |
| ■ read about and mention transshipment model by Moriari (sequential) . . . . .  | 31 |
| ■ revise compressor equations and add equations to nomenclature . . . . .   | 33 |
| ■ elaborate on different terms. . . . .   | 34 |
| ■ add derivative in appendix? . . . . .   | 34 |
| ■ explain model assumptions. . . . .  | 35 |
| ■ add graphic for tray measuremets. . . . .   | 37 |
| ■ write somewhere that stage indices will be omitted for convenience. . . . .   | 38 |
| ■ mention delft, sti, hydrodynamic continuum . . . . .  | 39 |
| ■ include Integrated condenser / reboiler unit . . . . .  | 39 |
| ■ check time constant (60) for flooding velocity . . . . .  | 42 |
| ■ check results for minimum column diameter when using flooding pressure drop, or fitted<br>flooding velocity . . . . .     | 42 |
| ■ which properties should be included? Or move everything to Appendix? . . . . .  | 46 |
| ■ include initial specifications in model structure . . . . .   | 49 |
| ■ include gPROMS code for IP's . . . . .  | 49 |
| ■ mention TP flashes branch of concentration sub-unit similar to adiabatic column, as all<br>streams are in equil.. . . . . | 49 |